

# ANALYSIS OF BUCK-BOOST CONVERTER APPLIED TO VARIOUS MPPT TECHNIQUES FOR PV SYSTEMS

P.GANGA<sup>1</sup>, R.SATHISH<sup>2</sup>

<sup>1</sup>Assistant Professor/EEE, Annapoorana Engineering College

<sup>2</sup>Assistant Professor/EEE, V.M.K.V Engineering College,

\*\*\*

**Abstract** - This paper proposes a comparative analysis between Buck and Boost DC-DC converters applied for Maximum Power Point Tracking (MPPT) techniques in a photovoltaic (PV) system. All experimental tests were carried out upon similar environmental conditions, steady solar irradiation and temperature, with maximum power point loads employed to extract all available power. The control of the PV system is evaluated by means of comparing three MPPTs techniques: Perturb and Observe, Temperature, and Incremental Conductance. In addition, MPPTs tracking factor and power conversion efficiency are investigated for each converter embedded with the re-spective technique. Finally, the experimental results are compared with the single-diode model approach, which shows the prominence of Boost converter using Perturb and Observe method.

**Key Words:** Boost, Buck, Single-Diode Model, Maximum Power Point Tracking Techniques, Photovoltaic System.

## 1. INTRODUCTION

Every year the world energy consumption has increased. For instance, from 2010 to 2014, a rise of 9.71% on the world total electricity production has been reported [1]. Due to this tendency, the need of renewable energies to supply the world demand follow the idea of sustainable development. In 2015, a growth about 147 GW on renewable energies was verified due to policies implemented by governments worldwide [2].

Photovoltaic (PV) generation systems, which are one of the green power sources available, have become popular due to several aspects: low operational costs; environmental friendly; inexhaustible operation; suitable to low power applications; and easy setup. The market response to these advantages shows that the global cumulative installed PV capacity has increased 25.4 % from 2014 to 2015 [3]. However, the main concern of PV energy is the low conversion efficiency, which rates from 14 % up to 18 % for commercial purposes, and reaches 35 % in research laboratories [4].

PV generation has a non-linear dynamic characteristic on its voltage and current output because of PV cells composition's [5]. Thus, there is only one combination of voltage and current where the maximum power relies. In addition, the uncertain environmental conditions puts the output power at different rates during the systems operation.

In order to obtain all available power provided by the PV module, Maximum Power Point Tracking (MPPT) techniques are usually employed [6]. They handle the PV operation by means of control algorithms applied to a power electronics interface, i.e. a DC-DC converter. Once the PV module conversion efficiency suffers from cost-competitiveness to be improved, an other way to optimize the PV system efficiency is by settling the right technique in a suitable power converter.

In the last decade, many MPPTs techniques have been researched: Constant Duty Cycle, Constant Voltage, Perturb and Observe, Incremental Conductance, Beta, System Oscillation, Ripple Correlation, Temperature, Fuzzy Logic, and Artificial Neural Network [7, 8]. Their main differences are related to speed, accuracy, and complexity, where three aspects of interest are usually evaluated: demands of PV module's physical informations, usage of computation capability, and efficiency.

Along with the MPPTs methods, a power electronic interface is mandatory. Different DC-DC converters topologies (Buck, Boost, Buck-Boost, Cuk, Sepic, and Zeta) have their own operational characteristics when applied to PV systems [9, 10]. Among these converters, Buck and Boost presents the most feasible sets, due to its high efficiency, simplicity, and low-order circuit [11].

Studies have already been developed in the field of PV systems in concern of MPPT and power electronics converters. Although, the analysis of MPPTs techniques with different power converters under the same experimental conditions still remains to be investigated in depth. The available studies usually fix a MPPT technique on multiple power converters, or, on the other hand, fix a power converter and do not take into account different types of MPPTs algorithms [12-14].

In order to contribute to the analysis above mentioned, this paper proposes an comparison between two non-isolated DC-DC converters (Buck and Boost) interfaced with three different MPPTs techniques (Perturb and Observe, Temperature, and Incremental Conductance) in a PV system. Experimental evaluations are carried out with the objective to match the best set of converter/technique conversion efficiency.

This paper is organized as follow: in section II a mathematical model of the PV module is described; section III presents the main characteristics of Buck and Boost DC-

DC converters; in section IV the Perturb and Observe, Temperature, and Incremental Conductance MPPT methods are clarified; and section V discusses about the simulation and experimental results. Finally, conclusions are contained in section VI.

## 2. MODELING OF PV MODULE

A practical PV module presents a nonlinear characteristic between its V-I curve, which depends mainly on the solar irradiation and temperature [15]. Based on the physical analysis of a PV cell, two equivalent electrical models can be built: the single-diode (Figure 1) and double-diode models. The former is widely used due to its combination of simplicity and accuracy [16]. For this reason, the single-diode model is adopted in this paper in order to have a efficiency comparison pattern.

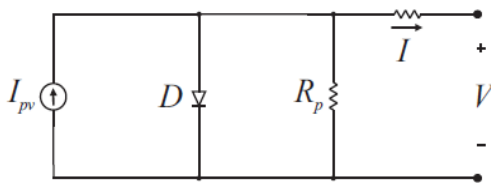


Fig. 1. Single-diode model representation of a PV cell.

The PV module output current can be described as [17]:

$$I = I_{pv} - I_D - I_{Rp} \tag{1}$$

$$I_{pv} = [I_{sc} + u_i \cdot (T - T_r)] \cdot \frac{S}{S_r} \tag{2}$$

$$I_D = \left[ \frac{(I_{sc} + u_i \cdot (T - T_r))}{e^{\frac{V_{oc} + u_v \cdot (T - T_r) \cdot q}{A \cdot k \cdot T \cdot n_s}} - 1} \right] \cdot \left[ e^{\frac{q \cdot [V + R_s \cdot I]}{A \cdot k \cdot T \cdot n_s}} - 1 \right] \tag{3}$$

$$I_{Rp} = \frac{V + R_s \cdot I}{R_p} \tag{4}$$

where  $I_{pv}$  is the current generated by the solar irradiation,  $I_D$  is the Shockley diode equation,  $I_{Rp}$  is the diode leakage current,  $I_{sc}$  is the short-circuit current,  $\mu_i$  is the short-circuit current temperature coefficient ( $A/^{\circ}C$ ),  $T$  is the cell temperature (Kelvin),  $T_r$  is the temperature in standard test conditions,  $S$  is the solar irradiation ( $W/m^2$ ),  $S_r$  is the solar irradiation in standard test conditions,  $V_{oc}$  is the open-circuit voltage,  $\mu_v$  is the open-circuit voltage temperature coefficient ( $V/^{\circ}C$ ),  $q$  is the electron charge ( $1.60217 \cdot 10^{-19}C$ ),  $k$  is the Boltzmann constant ( $1.3806 \cdot 10^{-23}J/K$ ),  $A$  is the diode ideality constant,  $n_s$  is the number of cells connected in series,  $V$  is the output voltage,  $I$  is the output current,  $R_s$  is the equivalent cell series resistance and  $R_p$  is the equivalent cell parallel resistance. Table I lists the characteristics of Kyocera KD 140SX PV module provided by the manufacturer, which one is used in this study. Its parameters are referred to the Standard Test Conditions (STC -  $25^{\circ}C$  and  $1000 W/m^2$ ) and Normal Operating Cell Temperature (NOCT -  $45^{\circ}C$  and  $800 W/m^2$ ). Unfortunately, some of the parameters

required to solve the single-diode model cannot be measured or found in the manufacturer's datasheet ( $R_p$ ,  $R_s$ ,  $A$ ). Therefore, mathematical approaches must be applied in order to determine these values.

## 3. DC-DC CONVERTERS

A PV system can only properly supply a load with the assistance of DC-DC converters. They have an essential part in this process, since all power goes through them. On the various converters usually used in PV systems, Buck and Boost gather one of the best solution sought by designers, simplicity and high efficiency [18]. In this way, the present section discusses the main aspects of these converters, while their exactly means of operation can be found easily in the present literature [11].

TABLE 1 Parameters of KD 140SX PV Module

Parameter	Label	STC	NOCT
Maximum Power	$P_{mpp}$	140 W	101 W
Voltage at $P_{max}$	$V_{mpp}$	17.7 V	16 V
Current at $P_{max}$	$I_{mpp}$	7.91 A	6.33 A
Open-circuit voltage	$V_{oc}$	22.1 V	20.2 V
Short-circuit current	$I_{sc}$	8.68 A	7.03 A
$V_{oc}$ temperature coefficient	$\mu_v$	$-0.08 V/^{\circ}C$	$-0.08 V/^{\circ}C$
$V_{mpp}$ temperature coefficient	$\mu_{V_{mpp}}$	$-0.0922 V/^{\circ}C$	$-0.0922 V/^{\circ}C$
$I_{sc}$ temperature coefficient	$\mu_i$	$0.00521 A/^{\circ}C$	$0.00521 A/^{\circ}C$
Number of cells in series	$n_s$	36	36
Efficiency	$\eta$	14 %	12.6 %

### A. Buck Converter

It is well known that, as a step down, Buck converter has its output voltage lower than its input voltage. This converter is widely used in regulated DC power supplies, motor speed control, and charging batteries [10].

As one of the Buck characteristics, the input current is chopped, producing high harmonic content and electromagnetic noise in near equipments. Also, the input power supply parasite inductance's can cause high voltage spikes on the semiconductor switch. In order to smooth this effect, an input filter can be included [19]. Figure 2 represents the main topology of Buck converter with an input filter.

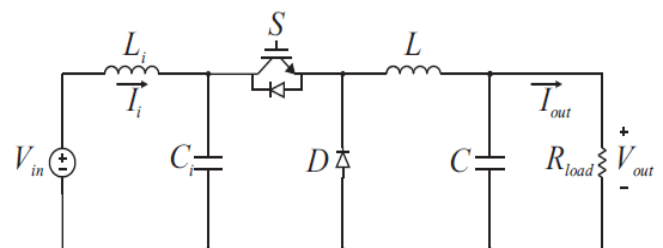


Fig. 2. DC-DC Buck converter with input filter.

## B. Boost Converter

In contrast to the step down converter, a step up topology, most known as Boost converter, is responsible for generating a higher output voltage than its input. Some of the main applications of this converter are in regulated DC power supplies and regenerative braking of DC motors [18]. The basic topology of Boost converter is shown in Figure 3.

## 4. MAXIMUM POWER POINT TRACKING SYSTEMS

In order to operate a PV system efficiently, it is mandatory to ensure that the maximum possible energy is extracted from the system at all time [20]. The PV module output power is dependent of solar irradiation and temperature, which are dynamic variables throughout the day. MPPT techniques are applied with the objective of maximum power extraction [21].

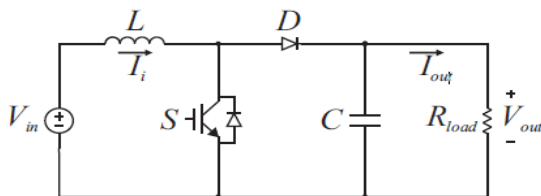


Fig. 3. DC-DC Boost converter.

Typically, the MPPT setup is achieved by interposing a DCDC converter between the PV module and the load. Thus, from the system measurements, the MPPT algorithm generates the optimal duty cycle in order to maintain the electrical quantities (voltage and current) at values near to the maximum power point [22]. Figure 4 shows a typical PV system scheme with maximum power point tracking.

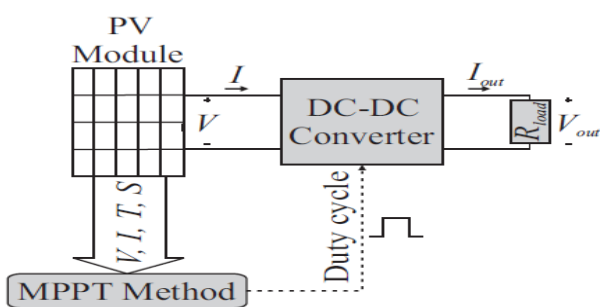


Fig. 4. PV system scheme with MPPT.

Approximately 40 various methods to track the maximum power point have already been compared in literature [8]. Among these, Perturbe and Observe (P&O), Temperature (Temp) and Incremental Conductance (InCond) are chosen for this study due to the following aspects: P&O and Temp methods have a simple setup, whereas Temp require physical PV module informations and P&O does not; InCond method presents higher tracking speed than P&O and Temp, although it needs more computance capability [23, 24].

## A. Perturbe and Observe

P&O method is widely used in commercial products due to its low-cost, simplicity, and ease of implementation [5]. However, this algorithm suffers from two drawbacks: the continuous oscillation around the maximum power point and the possibility of loosing its tracking direction when the solar irradiation increases rapidly. Both problems contribute for power losses and reduced tracking efficiency [25]. This technique is based on the duty cycle's perturbation and observing the effect on the output power. If this value is higher than its previous, then the algorithm keeps in the same direction of perturbation. Otherwise, the direction must be in the opposite way. When the maximum power point is reached, the tracking algorithm oscillates around it [26].

## B. Temperature

Temp is based on the theory that the output voltage is directly proportional to the temperature on the PV module surface [27], expressed as:

$$Vmpp(T) = Vmpp(Tr) + \mu v \cdot (T - Tr) \quad (5)$$

where  $Vmpp(T)$  is the maximum power point voltage and  $Vmpp(Tr)$  is the maximum power point voltage at STC. This method has a simple implementation and a good tracking factor. Although, a not uniform surface temperature or a wrong calibration of the temperature sensor may cause inaccurate tracking [24].

## C. Incremental Conductance

In order to reach the maximum power point (MPP), this method uses the slop of differential voltage  $dV$  and current  $dI$ , addressing the deficiency of P&O algorithm under variable irradiation conditions [21]. The output voltage and current from the PV module are monitored upon which the MPPT controller depends to calculate the conductance and incremental conductance to make its decision (increase or decrease the duty cycle) [22]. InCond aims to determine the voltage operating point at which the PV module instantaneous conductance ( $I/V$ ) is equal to the incremental conductance ( $dI/dV$ ). The slope is zero at MPP, positive on the left, and negative on the right [28].

## 5. RESULTS AND DISCUSSIONS

The experimental results presented in this section were accomplished to evaluate each converter versus MPPT technique. In this way, the results are divided in the following parts: single-diode model computational implementation; application of P&O, Temp, and InCond methods in both converters; and comparative analysis between converter/technique. Buck and Boost converters were designed based on [18] and [19]. Table II shows both DC-DC converters main parameters.

**TABLE 2** Parameters of Buck and Boost Converters

Parameters/Components	Buck	Boost
Input power ( $P_{in}$ )	100 W	100 W
Input voltage ( $V_{in}$ )	12-24 V	14-28 V
Output voltage ( $V_{out}$ )	12 V	28 V
Switching frequency ( $f_s$ )	30 kHz	30 kHz
$L_i, C_i$	24.77 $\mu H$ , 470 $\mu F$	-
$L, C$	240 $\mu H$ , 470 $\mu F$	653.3 $\mu H$ , 470 $\mu F$
Load resistance ( $R_{mpp}$ )	1.04 $\Omega$	5.6 $\Omega$

An experimental bench was developed to achieve the results. A pair of Tektronix MSO2014B Oscilloscope were used to acquire voltage, current, and solar irradiation measurements.

**A. Single-diode model**

computational implementation Due to the necessity of an efficiency comparison pattern, the ideal PV module KD 140SX model has been implemented by the single diode model through MATLAB software. The first step to solve the model was to determine all known parameters, which were given by the manufacturer datasheet, explicit in Table I. The unknown parameters ( $R_s$ ,  $R_p$ , and  $A$ )

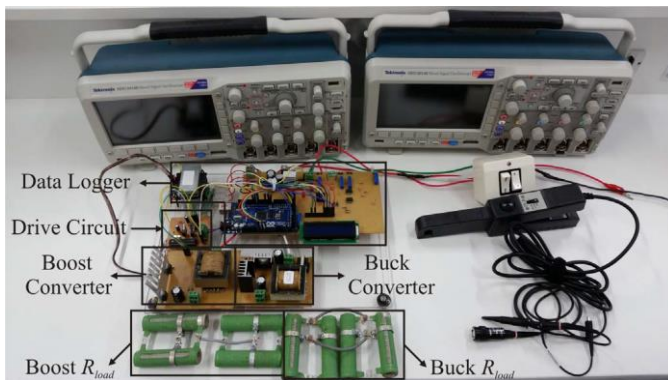


**Fig. 5.** Experimental bench.

were estimated by means of the non-linear least square technique using the Gauss-Newton numeric method. Considering an initial guess to the numeric method, typical values found in literature were assumed:  $R_s = 0.1\Omega$ ,  $R_p = 190\Omega$ , and  $A = 1.3$  [17]. After 19 iterations, the results for the numeric method of  $R_s$ ,  $R_p$ , and  $A$ , were, respectively, 0.1797  $\Omega$ , 190.0797  $\Omega$ , and 1.397. Equations (1), (2), (3), and (4) were plotted and compared with the manufacturer’s datasheet to validate the mathematical model and the applied numeric method (Figure 6). The average error was 4.8%, 3.32%, 3.3%, 0.88%, and 1.07% for the curves of 200 W/m<sup>2</sup> up to 1000 W/m<sup>2</sup>, respectively.

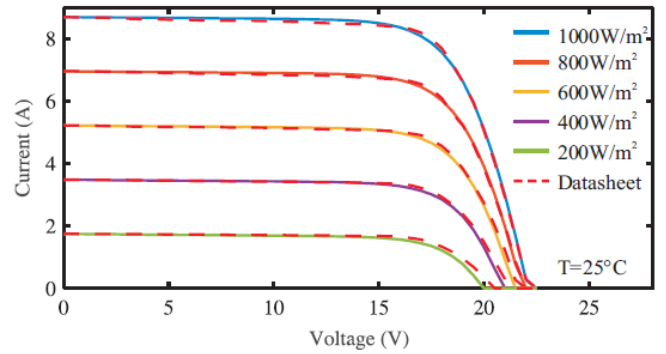


**Fig. 6.** Comparison between the implemented mathematical method and the manufacturer’s datasheet.

**B. MPPT algorithms implementation**

In order to perform the proposed MPPT algorithms, it is necessary to set up a system able to measure PV module voltage and current, as well as the irradiation and temperature conditions. For this purpose, a data acquisition system (data logger) was developed using the ATmega2560 microcontroller. Certificated instruments with traceability were used to accomplish a data logger with variations less than 5 %. The voltage and current circuits were calibrated with a Fluke 117 multimeter. A type K Termopar was used to compare the PV surface temperature with the digital sensor DS18B20. Finally, the piranometer (irradiation sensor) was compared with the solar meter TES 1333R. A drive platform was developed to acquire the measurements from the data logger and perform the respective MPPT algorithm acting on the converter’s duty cycle. This circuit was based on the microcontroller ATmega328/P and the halfbridge driver IR2104. The methods tracking frequencies were determined as 0.5 Hz due to the slow environmental changing conditions. Also, the duty cycle’s step were fixed in 3 % for both converters.

**C. Comparative analysis between Buck/Boost converters and P&O/Temp/InCond MPPT methods**

Aiming the best set of converter/technique, the experimental bench has worked from 13 PM to 15:30 PM on 5/22/2017. During the tests, the solar irradiation presented a constant behavior ( $S_{avg}$ ) with a steady temperature ( $T_{avg}$ ). Figures 7-12 depicts the measurements for each converter/ technique during 80 seconds, with a time step of 0.016 seconds. To smooth the noise, a 3 samples moving average filter has been applied through MATLAB software.

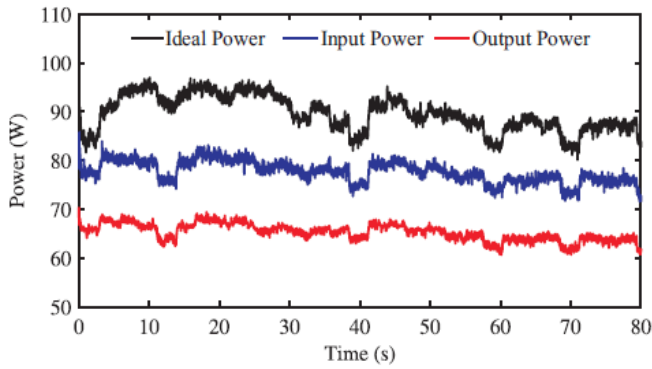


Fig. 7. Buck converter operating with P&O MPPT method.  
 $S_{avg} = 708.58 \text{ W/m}^2, T_{avg} = 37.05^\circ\text{C}$

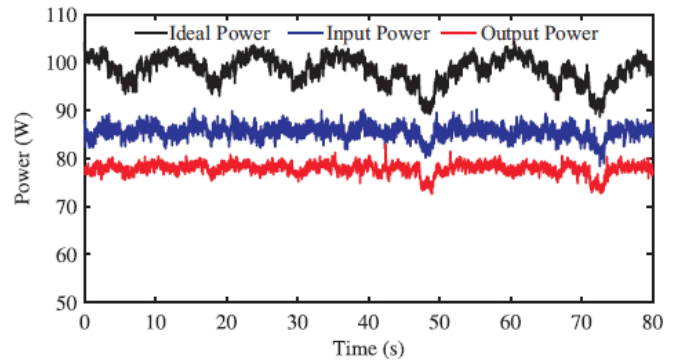


Fig. 10. Boost converter operating with P&O MPPT method.  
 $S_{avg} = 800.59 \text{ W/m}^2, T_{avg} = 40.00^\circ\text{C}$

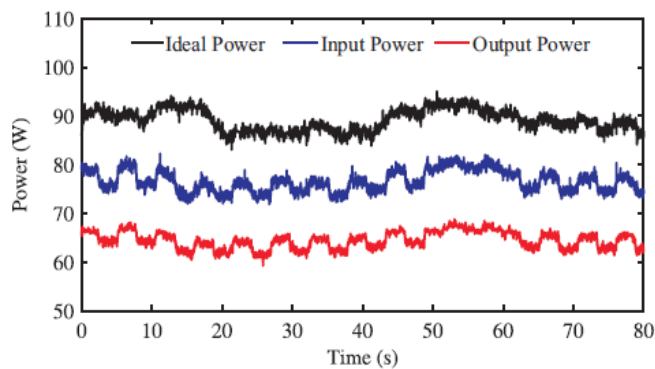


Fig. 8. Buck converter operating with Temp MPPT method.  
 $S_{avg} = 696.08 \text{ W/m}^2, T_{avg} = 37.10^\circ\text{C}$

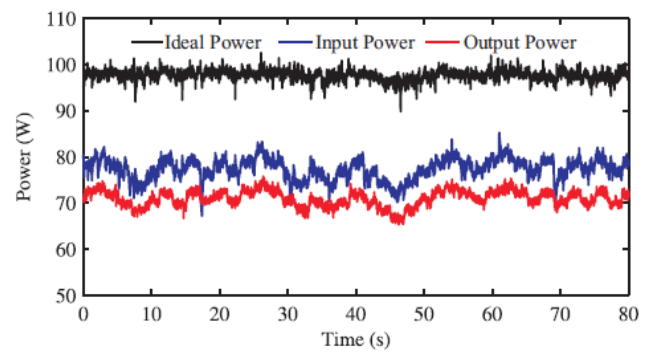


Fig. 11. Boost converter operating with Temp MPPT method.  
 $S_{avg} = 768.57 \text{ W/m}^2, T_{avg} = 39.35^\circ\text{C}$

The performance of P&O, Temp, and InCond MPPTs techniques reveal the expected behavior throughout the tests for a steady irradiation and temperature. Figures 7 and 10 present a continues oscillation, which is an inherent characteristic of P&O. Temp algorithm performed with low power oscillation, but its operational point was farther from MPP than the others (Figures 8 and 11). Finally, in Figures 9 and 12, InCond technique evidence a better control of converter's duty cycle. In order to compare the systems efficiencies, the factors to be analyzed are: MPPTs algorithms tracking factor (TF)

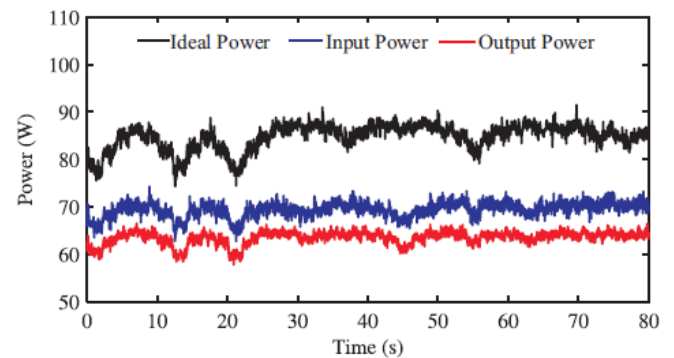


Fig. 12. Boost converter operating with InCond MPPT method.  
 $S_{avg} = 679.33 \text{ W/m}^2, T_{avg} = 38.30^\circ\text{C}$

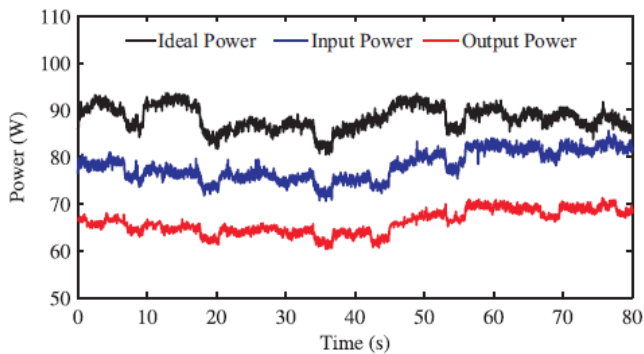


Fig. 9. Buck converter operating with InCond MPPT method.  
 $S_{avg} = 701.15 \text{ W/m}^2, T_{avg} = 37.62^\circ\text{C}$

As a result of a Rmpp implementation to operate at the PV module MPP, Buck and Boost have failed to track it efficiently, showing suboptimal operations in the respective conditions. Even though this concept has been reported in literature [10, 28, 29], this paper has presented, by means of experimental results, its efficiency rates. Therefore, to improve the methods TF in both converters, different loads will be applied: load less than Rmpp for Buck and load greater than Rmpp for Boost.

## 6. CONCLUSION

This paper presented an experimental bench development in order to evaluate P&O, Temp, and InCond MPPTs techniques applied to Buck and Boost power converters. The results of Rmpp load appliance showed that Boost was 7.13 % more efficiently in power conversion than Buck. In this context, Boost/P&O setup performed the higher power conversion efficiency. Finally, it is possible to observe the limitations of Buck and Boost converters when applied to MPPTs systems, whereas, its loads and order must be taken into account.

## REFERENCES

- [1] International Energy Agency. World Energy Statistics (2016 edition). Paris, France, 2016.
- [2] Janet L. Sawin, Kristin Seyboth, and Freyr Sverrisson. Renewables 2016: Global Status Report. Paris, 2016.
- [3] Fraunhofer Institute of Solar Energy Systems. Photovoltaics report. Technical Report November, Fraunhofer Institute for Solar Systems Energy, Freiburg, 2016.
- [4] Tatsuya Takamoto, Takaaki Agui, Atsushi Yoshida, Katsuya Nakaido, Hiroyuki Juso, Kazuaki Sasaki, Kazuyo Nakamura, Hiroshi Yamaguchi, Tomoya Kodama, Hidetoshi Washio, Mitsuru Imaizumi, and Masato Takahashi. World's highest efficiency triple-junction solar cells fabricated by inverted layers transfer process. Conference Record of the IEEE Photovoltaic Specialists Conference, pages 412–417, 2010.
- [5] [5] Nicola Femia, Giovanni Petrone, Giovanni Spagnuolo, and Massimo Vitelli. Power Electronics and Control Techniques for Maximum Energy Harvesting in Photovoltaic Systems. CRC Press, New York, 1 edition, 2013.
- [6] Kashif Ishaque, Zainal Salam, Muhammad Amjad, and Saad Mekhilef. An improved particle swarm optimization (PSO)-based MPPT for PV with reduced steady-state oscillation. IEEE Transactions on Power Electronics, 27(8):3627–3638, 2012.
- [7] Moacyr A. G. De Brito, Luigi G. Junior, Leonardo P. Sampaio, Guilherme A. Melo, and Carlos A. Canesin. Main maximum power point tracking strategies intended for photovoltaics. COBEP 2011 - 11th Brazilian Power Electronics Conference, pages 524–530, 2011.
- [8] Deepak Verma, Savita Nema, A. M. Shandilya, and Soubhagya K. Dash. Maximum power point tracking (MPPT) techniques: Recapitulation in solar photovoltaic systems. Renewable and Sustainable Energy Reviews, 54:1018–1034, 2016.
- [9] Soediby, Amri Budi, and Mochamad Ashari. The Comparative Study of Buck-Boost, Cuk, Sepic and Zeta Converters for Maximum Power Point Tracking Photovoltaic Using P&O Method. In 2nd Int. Conference on Information Technology, Computer and Electrical Engineering (ICITACEE), pages 327–332, 2015.
- [10] G. Dileep and Singh S.N. Selection of non-isolated DCDC converters for solar photovoltaic system. Renewable and Sustainable Energy Reviews, 76:1230–1247, 2017.
- [11] Maria B. F. Prieto, Salvador P. Litr'an, Eladio D. Aranda, and Juan M. E. G'omes. New Single-Input, Multiple-Output Converter Topologies. IEEE Industrial Electronics Magazine, 10(2):6–20, 2016.
- [12] Rashmi, J. Manohar, and K. S. Rajesh. A Comparative Study and Performance Analysis of Synchronous SEPIC Converter and Synchronous Zeta Converter by using PV System with MPPT Technique. In 1st IEEE International Conference on Power Electronics, Intelligent Control and Energy Systems (ICPEICES-2016), Dheli, 2016.
- [13] Mustafa E. Basoglu and Bekir Cakir. Hardware based comparison of buck-boost converter topologies in MPPT systems. In 9th International Conference on Electrical and Electronics Engineering, pages 1109–1112, 2015.
- [14] Sachin K. Singh and Ahteshamul Haque. Performance evaluation of MPPT using boost converters for solar photovoltaic system. In 12th IEEE International Conference Electronics, Energy, Environment, Communication, Computer and Control, New Delhi, 2016.
- [15] Emerson A. Silva, Fabricio Bradaschia, Marcelo C. Cavalcanti, and Aguinaldo J. Nascimento. Parameter Estimation Method to Improve the Accuracy of Photovoltaic Electrical Model. IEEE Journal of Photovoltaics, 6(1):278–285, 2016.
- [16] Marcelo G. Villalva, Jonas R. Gazoli, and E. Ruppert Filho. Modeling and circuit-based simulation of photovoltaic arrays. Brazilian Power Electronics Conference, pages 1244–1254, 2009.
- [17] Marcelo G. Villalva, Jonas R. Gazoli, and Ernesto R. Filho. Comprehensive approach to modeling and simulation of photovoltaic arrays. IEEE Transactions on Power Electronics, 24(5):1198–1208, 2009.
- [18] Ned Mohan, Tore M. Undeland, and William P. Robbins. Power Electronics: Converters, Applications, and Design. JohnWiley & Sons, Inc, New York, 3 edition, 2002.
- [19] Denizar C. Martins and Ivo Barbi. Eletrônica de Potência: conversores CC-CC básicos não isolados. Ed. dos Autores, Florianópolis, 2 edition, 2006.

- [20] S. Lyden and M. E. Haque. Maximum Power Point Tracking techniques for photovoltaic systems: A comprehensive review and comparative analysis. *Renewable and Sustainable Energy Reviews*, 52:1504–1518, 2015.
- [21] Muhammad H. Uddin, Muhammad A. Baig, and Muhammad Ali. Comparison of 'Perturb & Observe' and 'Incremental Conductance', Maximum Power Point Tracking algorithms on real environmental conditions. In *International Conference on Computing, Electronic and Electrical Engineering*, pages 313–317, 2016.
- [22] Boualem Bendib, Hocine Belmili, and Fateh Krim. A survey of the most used MPPT methods: Conventional and advanced algorithms applied for photovoltaic systems. *Renewable and Sustainable Energy Reviews*, 2015.
- [23] Moacyr A. G. De Brito, Luigi Galotto, Leonardo P. Sampaio, Guilherme A. Melo, and Carlos A. Canesin. Evaluation of the main MPPT techniques for photovoltaic applications. *IEEE Transactions on Industrial Electronics*, 60(3):1156–1167, 2013.
- [24] Pallavee Bhatnagar and R. K. Nema. Maximum power point tracking control techniques: State-of-the-art in photovoltaic applications. *Renewable and Sustainable Energy Reviews*, 23:224–241, 2013.
- [25] Jubaer Ahmed and Zainal Salam. A Modified P&O Maximum Power Point Tracking Method with Reduced Steady State Oscillation and Improved Tracking Efficiency. *IEEE Transactions on Sustainable Energy*, 3029:1–10, 2016.
- [26] L. Bouselham, B. Hajji, and H. Hajji. Comparative study of different MPPT methods for photovoltaic system. In *3rd International Renewable and Sustainable Energy Conference*, pages 1–5, Marrakech, 2015.
- [27] Roberto F. Coelho, Filipe M. Concer, and Denizar C. Martins. A MPPT Approach Based on Temperature Measurements Applied in PV Systems. *9th IEEE/IAS International Conference on Industry Applications*, 2010.
- [28] Makbul A. M. Ramli, Ssennoga Twaha, Kashif Ishaque, and Yusuf A. Al-Turki. A review on maximum power point tracking for photovoltaic systems with and without shading conditions. *Renewable and Sustainable Energy Reviews*, 67:144–159, 2017.
- [29] Barnam J. Saharia, Munish Manas, and Subir Sen. Comparative study on buck and buck-boost DC-DC converters for MPP tracking for photovoltaic power systems. In *2nd International Conference on Computational Intelligence and Communication Technology*, pages 382–387, 2016.